Thermal and Material Transfer in Turbulent Gas Streams: One-Inch Spheres

EMILIO VENEZIAN, MANUEL J. CRESPO, and B. H. SAGE

California Institute of Technology, Pasadena, California

As part of a study of the effect of conditions of flow upon macroscopic and local thermal and material transport from spheres, an investigation was made of the macroscopic and local transport from a silver and a porous sphere each 1 in. in diameter. The transport was measured in a turbulent air stream at Reynolds numbers up to 7,500, and the apparent level of longitudinal turbulence of the stream was varied between 0.013 and 0.15. In the case of the porous sphere the thermal and material transport were evaluated for the evaporation of *n*-octane.

The results indicate that the macroscopic Nusselt number is substantially larger for combined thermal and material transport than for thermal transport alone. The local Nusselt number varied by a factor of 5 around the silver sphere from stagnation to separation.

The thermal and material transport from spheres has been the subject of experimental investigation for many years. Recently Brown (2, 3) reviewed the available experimental and theoretical treatments for both macroscopic and local material transport, and Sato (*16*) and Short (*17*) presented similar reviews of the thermal transfer from spheres. To avoid repetition no general review of earlier experimental work is given, although reference is made to it in the ensuing discussion.

The current experimental investigation involved evaluation of macroscopic and local thermal and material transport around a porous and a silver sphere 1 in. in diameter. Measurements were made at Reynolds numbers between 2,000 and 7,500 and at apparent levels of turbulence between 0.013 and 0.15. The local transport was determined from the temperature gradients in the boundary flows.

No measurement of the microscopic nature of the turbulent field was made because this would have involved a study of equal or greater magnitude than the present work. The present experimental work supplements and extends studies (*2, 3, 16, 17*) carried out with 0.5-in. spheres. It also permits comparison of the accuracy of the linear methods employed in predicting the effect of the size of the sphere on the local thermal and material transport. Such comparative information is not often available for the same intensities and scale of turbulence.

METHODS AND EQUIPMENT

The present investigation was carried out by supporting a porous and a silver sphere in a turbulent air stream and by measuring the associated thermal or material transport. In the case of the porous sphere the rate of evaporation of *n*-octane was measured, and in the case of the silver sphere the electrical power required to maintain the surface of the sphere at a predetermined steady temperature was established. The temperature distribution in the air stream around the silver sphere was measured with a platinum, platinum-rhodium thermocouple, 0.0003 in. in diameter, mounted upon a probe (*11*). Information concerning the distribution of thermocouple temperature about the sphere was obtained for a number of different conditions of flow. The effect of separation at polar angles of the order of 100 deg. from stagnation was evident.

The equipment used to supply the air has been described in detail (*10*). The velocity of the stream was established (*11*) within 0.5% and remained steady within 0.2% during a particular investigation. The temperature of the air stream was known within 0.1°F. relative to the international platinum scale (*10*).

In order to increase the level of turbulence a steel plate 0.1875 in. thick, having holes 0.875 in. in diameter on 1.0-in. centers, was inserted in the air stream near the exit of a rectangular conduit. Sections of steel duct, 3 by 12 in. in cross section, in lengths varying between 3 and 12 in. were placed on the downstream side of the perforated plate. In evaluating the apparent level of turbulence the data of Davis (*5, 6*) were employed. The interpretation of his results in terms of behavior in the wake of the perforated plate has been described (*17*). However some uncertainties are involved in this interpretation. The level of turbulence is usually defined as the quotient of the root mean square of the fluctuating velocities and the gross velocity. Davis (*5, 6*) reported both transverse and longitudinal turbulence levels. Since the physical arrangement of the grid and ductwork differ slightly from those used by Davis, the term *apparent level of turbulence* has been used to represent the level of turbulence, predicted from Davis' experiments at the same downstream positions measured from the

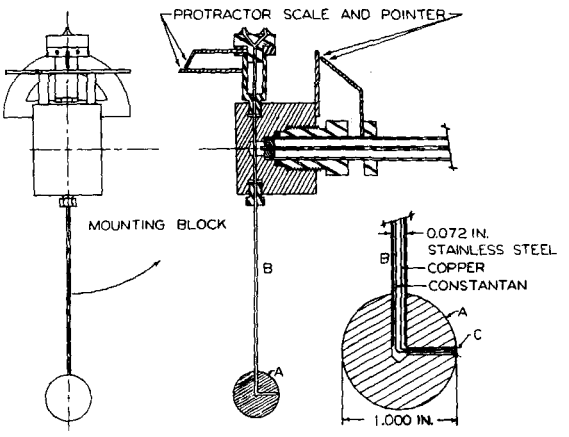

Fig. 1. One-inch porous sphere assembly.

TABLE 1. EXPERIMENTAL CONDITIONS

Test no.	Pressure, lb./sq. in. abs.	Air temperature, °F.	Gross air velocity, ft./sec.	Weight fraction water	Apparent level of turbulence fraction	Downstream distance from grid, in.	Total evaporation rate, lb./sec.
			1.0-in. porous sphere				
303	14.367	100.15	4.04	0.0058	0.013	No grid	4.273×10^{-6}
310	14.358	100.15	4.05	0.0100	0.013	No grid	4.399
328	14.290	100.11	4.07	0.0092	0.013	No grid	4.243
310	14.380	100.15	8.03	0.0098	0.013	No grid	6.014
306	14.369	100.13	8.04	0.0087	0.013	No grid	6.072
307	14.352	100.17	8.04	0.0062	0.013	No grid	6.121
305	14.340	100.13	8.05	0.0072	0.013	No grid	6.139
327	14.308	100.07	8.07	0.0097	0.013	No grid	6.059
322	14.284	100.15	8.07	0.0073	0.013	No grid	6.025
326	14.274	100.02	8.09	0.0089	0.013	No grid	6.099
311	14.254	100.13	15.77	0.0104	0.013	No grid	8.561
317	14.273	100.15	4.07	0.0083	0.071	10.112	4.321
316	14.315	100.07	8.08	0.0109	0.067	10.307	6.262
314	14.248	99.78	8.07	0.0063	0.067	10.109	6.356
318	14.159	100.11	16.41	0.0092	0.065	10.107	8.984
313	14.301	100.11	4.13	0.0061	0.094	7.163	4.340
314	14.270	100.15	8.07	0.0067	0.092	7.166	6.356
312	14.244	100.13	15.86	0.0104	0.087	7.159	8.973
320	14.333	100.13	4.05	0.0064	0.149	4.194	4.758
321	14.336	100.15	8.03	0.0072	0.147	4.183	7.321
319	14.228	100.11	16.34	0.0082	0.133	4.197	11.088
			1.0-in. silver sphere				
176A	14.270	100.54	4.07	0.120	0.013	No grid	
177	14.311	99.87	4.08	0.126	0.013	No grid	
176B	14.302	100.54	8.08	0.120	0.013	No grid	
174	14.323	100.02	16.23	0.123	0.013	No grid	
186	14.328	100.00	8.05	0.0150	0.054	13.21	
185	14.298	100.15	16.21	0.0092	0.051	13.22	
183	14.304	99.81	8.10	0.0148	0.067	10.37	
184	14.283	100.13	16.32	0.0120	0.064	10.18	
182	14.497	100.09	8.06	0.0115	0.091	7.23	
181	14.322	100.09	16.09	0.0107	0.086	7.24	
178	14.292	100.11	4.07	0.0139	0.151	4.27	
179	14.350	100.04	8.07	0.0181	0.143	4.26	
180	14.357	100.19	16.22	0.0126	0.132	4.28	

perforated plate. The downstream distance from the perforated plate also is included on a diagram. In effect the apparent level of turbulence is used as an approximate evaluation of the level of turbulence and is a single-valued function of the downstream distance from the perforated plate.

Figure 1 shows details of the porous sphere assembly. The porous sphere A which was composed of diatomaceous earth, was supported by a stainless steel tube B used for the injection of *n*-octane. The arrangement for support of the sphere permitted the use of a single thermocouple C to determine the distribution of temperature on the surface of the sphere. The sphere could be rotated and the angle of attack of the supporting tube changed. A copper-constantan thermocouple 0.003 in. in diameter was used. A capillary manometer measured the capillary pressure of the wetted porous sphere. It was used to determine that the injector (*10, 12*) which supplied *n*-octane was delivering fluid at the same rate that it was evaporating from the sphere. The entire assembly shown in Figure 1 was mounted upon traversing gear (*2*).

Details of construction of the silver sphere are shown in Figure 2. A copper sphere was prepared with a continuous spiral groove within which an insulated electric heater was wound. The sphere was covered with two silver hemispherical shells soldered in place. The entire assembly was supported by a 0.094 in. stainless steel tube. Copper-constantan thermocouples 0.003 in. in diameter were located at four positions as shown in Figure 2. With this arrangement it was not necessary to rotate the sphere as had been done with the porous sphere which used a single thermocouple. Guard heaters were attached to the supporting tube in order to avoid thermal transport. Some difficulty was experienced from oscillation of the sphere when it was supported in the air stream in any but a vertical angle of attack. It was found that by attaching small weights to the supporting tube in various positions at least 4 diam. away from the sphere this difficulty could be eliminated at all the velocities investigated.

MATERIALS

Pure grade n-octane was obtained which weighed 43.6475 lb./cu. ft. at 77°F. as compared with a value of 43.604 lb./cu. ft. reported for an air-saturated sample by Rossini (*15*). The index of refraction to the D-lines of sodium at 77°F. was 1.39532, as compared with a value of 1.39505 reported by Rossini (*15*) for an air-saturated sample. The supplier indicated that this sample contained less than 0.01 mole fraction material other than *n*-octane, and the agreement of the foregoing measurement of values of specific weight and index of refraction with accepted critically chosen values (*15*) confirms these indications. It is desirable to utilize relatively pure materials in such an investigation because otherwise the less volatile impurities accumulate in substantial amounts on the evaporating surface of the porous sphere.

ANALYSIS

Details of the analysis of thermal transfer (*17*) and material transfer from spheres (*3*) are available. A brief review of the analysis follows. In the case of material transport the local thermal flux may be related to the local material flux by the following equation:

$$\dot{Q} = -\dot{m}_k (H_{g,t,k} - H_{l,t,k}) =$$

$$-\dot{m}_k[L_k + C_{p,l,k}(t_t - t_{l,t})] \quad (1)$$

When Equation (1) is applied to the actual situation associated with the entire sphere, there is obtained

$$\dot{Q} = \{-\dot{m}_k [L^*_k + C_{p,l,k}(t^*_t - t_{l,t})] - \dot{Q}_t - \dot{Q}_r\} \frac{A_{sp}}{A_{sp} - A_t}$$

$$= \{ -\dot{m}_k[L^*_k + C_{p,l,k}(t^*_t - t_{l,t})] + \left[(k_l A_l + k_t A_t + k_w A_w) \left(\frac{\partial t_t}{\partial x}\right)_{r=o} \right] - \left[A_{sp}\beta (T_t^{*4} - T_{sr}^{*4}) \left(1 \Big/ \left(\frac{1}{\epsilon_{sp}} + \frac{1}{\epsilon_{sr}} - 1\right)\right)\right]\} \frac{A_{sp}}{A_{sp} - A_t} \quad (2)$$

The first equality relates the total thermal flux to the total weight rate of evaporation with appropriate correction for the thermal flux in the sup-

porting tube and for radiation. The second equality indicates the approach employed in evaluating these two correction terms. In Equation (2) the quantity $A_{sp}/(A_{sp} - A_i)$ represents a first-order correction to the gross transport as a result of the presence of the supporting tube. In the above quantity A_{sp} is the area of the sphere uncorrected for the supporting tube. The corrected values present the total thermal flux that would have existed if the supporting tube had not been present. Such a simple method of correction assumes that the local thermal flux at the point where the sphere is supported by the tube is equal to the average thermal flux around the sphere. Such a situation is approximated in the current study. The quantity $A_{sp}/(A_{sp} - A_i)$ had a value of 1.0013 for the porous sphere.

The total thermal flux from the 1.0-in. silver sphere was obtained from

$$\overset{\circ}{\mathbf{Q}} = \underline{\overset{\circ}{\xi}_i}^* = \frac{[\int_o^{\theta_e} EId\theta]}{\theta_e} \frac{A_{sp}}{A_{sp} - A_i} \qquad (3)$$

The correction for the area of the supporting tube $A_{sp}/(A_{sp} - A_i)$ is 1.0022 for the silver sphere. In this instance a correction for thermal flux along the supporting tube was not necessary, nor was there any need for a radiation correction because the emissivity of the silver sphere was low.

For both the porous and silver spheres the macroscopic heat transfer coefficient h^*, the macroscopic Nusselt number based on interfacial properties $N^*_{Nu_i}$, and the Reynolds number based upon the properties in the free stream N_{Re_∞} were evaluated as follows:

$$h^* = \overset{\circ}{\mathbf{Q}}/A_i(t_i^* - t_\infty) \qquad (4)$$

$$N^*_{Nu_i} = h^* \mathbf{d}/k_i = (\overset{\circ}{\mathbf{Q}}\,\mathbf{d})/[k_i A_i(t_i^* - t_\infty)] \qquad (5)$$

In the foregoing equation the subscript i refers to conditions at the interface:

$$N_{Re_\infty} = \mathbf{d}\, U_\infty/\nu_\infty \qquad (6)$$

The average temperature at the interface was obtained from

$$t_i^* = [\int_o^A t_i\, d\, A_i]/A_i \qquad (7)$$

The values of the macroscopic interfacial Nusselt number were calculated, and plotted, and smoothed as a function of Reynolds number and apparent level of turbulence. It was not found feasible to compute corresponding values of the macroscopic Sherwood number. No information concerning the molecular transport of n-octane in air was available. The compressibility factor and the ratio of fugacity to pressure of the air-*n*-octane mixtures were unknown. At such time as experimental information concerning the molecular equilibrium and molecular transport properties of mixtures of *n*-octane and air in the gas phase is available, the current data will permit calculation of Sherwood numbers and similar transport characteristics.

TABLE 2. THERMAL AND MATERIAL TRANSPORT

Test no.	Reynolds number free stream	Average surface temperature, °F.	Total thermal transfer, B.t.u./sec. uncorrected*	Total thermal transfer, B.t.u./sec. corrected†	Macroscopic Nusselt number surface uncorrected*	Macroscopic Nusselt number surface corrected†	$N^*_{Nu_i}/N^{1/2}_{Re_\infty}$
			1.0-in. porous sphere				
303	1,822	79.94	0.6395×10^{-3}	0.5762×10^{-3}	30.31	27.30	0.6396†
310	1,824	79.91	0.6589	0.5992	31.17	28.35	0.6381
328	1,825	79.81	0.6348	0.5716	29.96	26.97	0.6313
310	3,626	79.60	0.8961	0.8349	41.76	38.92	0.6463
306	3,625	79.39	0.9045	0.8451	41.82	39.02	0.6481
307	3,621	79.37	0.9118	0.8400	41.99	38.69	0.6430
305	3,625	79.12	0.9141	0.8577	41.68	39.11	0.6496
327	3,625	78.89	0.9018	0.8458	40.78	38.25	0.6353
322	3,620	79.50	0.8976	0.8248	41.63	38.25	0.6352
326	3,624	78.92	0.9077	0.8469	41.24	38.44	0.6385
311	7,056	79.39	1.2717	1.2049	58.72	55.65	0.6625
317	1,823	80.63	0.6462	0.5950	31.75	29.20	0.6839
316	3,632	79.69	0.9354	0.8799	43.99	41.34	0.6859
314	3,615	79.56	0.9453	0.8847	44.77	41.91	0.6970
318	7,294	79.41	1.3326	1.2691	61.65	58.72	0.6875
313	1,852	80.37	0.6485	0.5998	31.46	29.10	0.6762
314	3,615	79.56	0.9452	0.8839	43.97	41.11	0.6837
312	7,092	79.21	1.3299	1.2671	60.87	58.01	0.6888
320	1,822	80.51	0.7100	0.6546	34.66	31.96	0.7487
321	3,613	79.67	1.0870	1.0169	50.83	47.55	0.7911
319	7,299	79.40	1.6414	1.5768	75.91	72.93	0.8536
			1.0-in. silver sphere				
176A	1,880	160.1	2.3371×10^{-3}		22.2		0.5120**
177	1,884	159.8	1.632		22.0		0.5069
176B	3,730	160.0	2.3371		31.4		0.5141
174	7,500	160.2	3.3179		44.5		0.5138
186	3,715	160.2	2.4155		32.4		0.5136
185	7,480	160.0	3.4785		46.9		0.5423
183	3,740	160.0	2.3821		32.0		0.5233
184	7,530	160.2	3.5811		48.1		0.5543
182	3,720	160.2	2.4659		33.2		0.5443
181	7,430	160.3	3.6016		48.3		0.5603
178	1,880	160.0	1.8557		25.0		0.5766
179	3,720	160.2	2.8578		38.4		0.6296
180	7,490	160.3	4.3481		58.5		0.6759

* Uncorrected for radiant transport.
† Corrected for radiant transport.
** No radiation correction required.

Local Transport

The local temperature at the surface of the porous sphere was normalized with the following expression:

$$\Upsilon_i = (t_i - t_\infty)/(t_{eq} - t_\infty) \qquad (8)$$

The local normalized surface temperature was smoothed with respect to polar angle, level of turbulence, and Reynolds number, and from this the corresponding values of local surface temperature were obtained by rearrangement of Equation (8). The differences in temperature from point to point on the silver sphere were sufficiently small as to permit the use of a simple surface average.

A relative local transport, defined as the ratio of the local Nusselt number to the macroscopic Nusselt number, was obtained as follows:

$$\frac{N_{Nu_i}}{N^*_{Nu_i}} = \frac{\left(\frac{\partial t}{\partial r}\right)_{i,\psi} \int_o^A (t_i - t_\infty) d\, A_i}{(t_i - t_\infty) \int_o^A \left(\frac{\partial t}{\partial r}\right)_{i,\psi} d\, A_i}$$

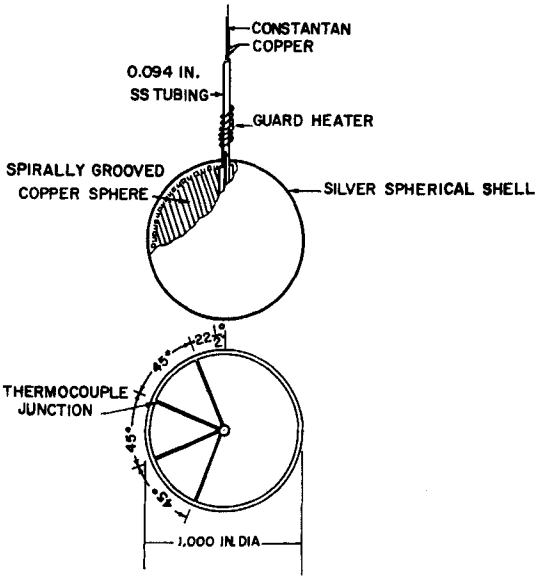

Fig. 2. One-inch silver sphere assembly.

$$= \frac{(t_i^* - t_\infty)\left(\frac{\partial t}{\partial r}\right)_{i,\psi}}{(t_i - t_\infty)\left(\frac{\partial t}{\partial r}\right)^*_{i,\psi}} \qquad (9)$$

In the derivation of Equation (9) it is assumed that the thermal conductivity is independent of variations in the local temperature. It is noted that Equation (9) involves values of the derivative of the air temperature with respect to radius at the interface. The methods of arriving at the corrections to the measured change in thermocouple temperature with radius have been described in detail (*1, 17*). In evaluating the relative local transport given by Equation (9) the corrections described (*1, 17*) were applied to the measured wire temperature gradients. In the evaluation of the air temperature gradients at the surface of the sphere from the associated wire temperature gradients uncertainties of not more than 2% were introduced.

EXPERIMENTAL RESULTS

The experimental conditions for the measurements upon the porous and silver spheres are set forth in Table 1. The test numbers indicated are used in subsequent discussion to identify each set of experimental conditions. Table 2 presents derived information, including the free stream Reynolds number and the average surface temperature as evaluated by Equation (7), as well as the total thermal transfer and the macroscopic Nusselt number corrected and uncorrected for radiation. In the case of the silver sphere there was no occasion to correct for the effect of radiant transport because it was negligible. In addition the quotient of the macroscopic Nusselt number and the square root of the Reynolds number are included.

The experimental values of the macroscopic Nusselt number are shown as a function of apparent level of turbulence in Figure 3, for both the porous and silver spheres. For the porous sphere the values of Nusselt number corrected for radiant transport are illustrated. As was found in earlier studies (*2, 3*) the Nusselt number for the same level of turbulence and Reynolds number is larger with combined thermal and material transport than it

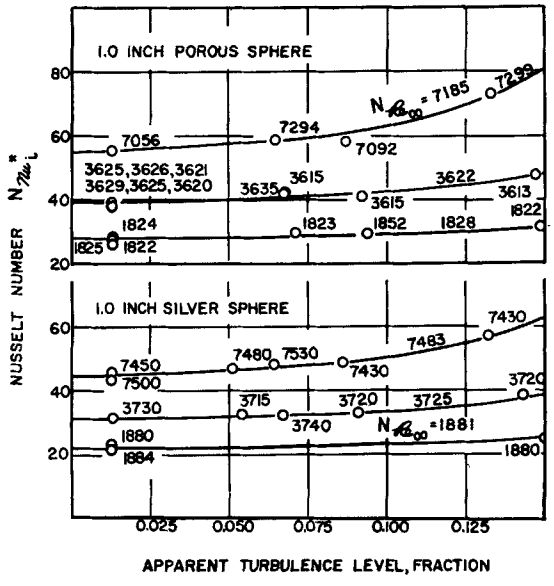

Fig. 3. Macroscopic thermal transport for 1-in. silver and porous spheres.

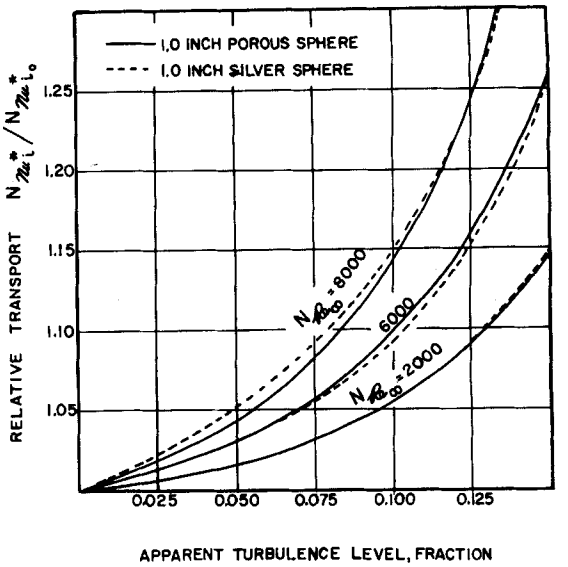

Fig. 4. Relative macroscopic thermal transport for 1-in. silver and porous spheres.

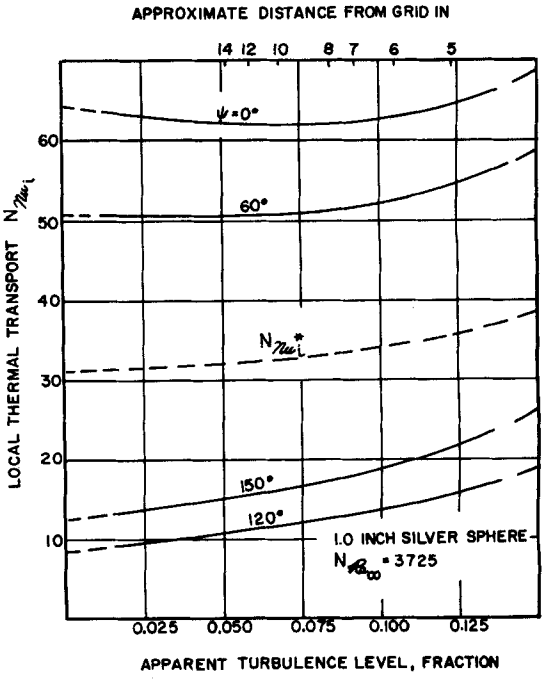

Fig. 5. Local thermal transport for 1-in. silver sphere.

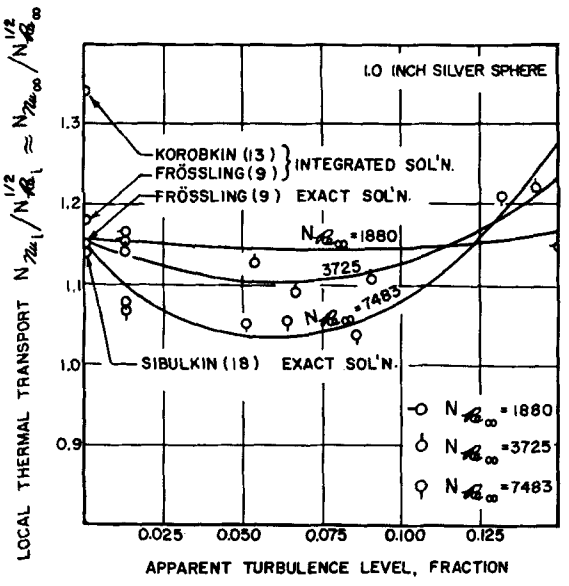

Fig. 6. Local thermal transport at stagnation.

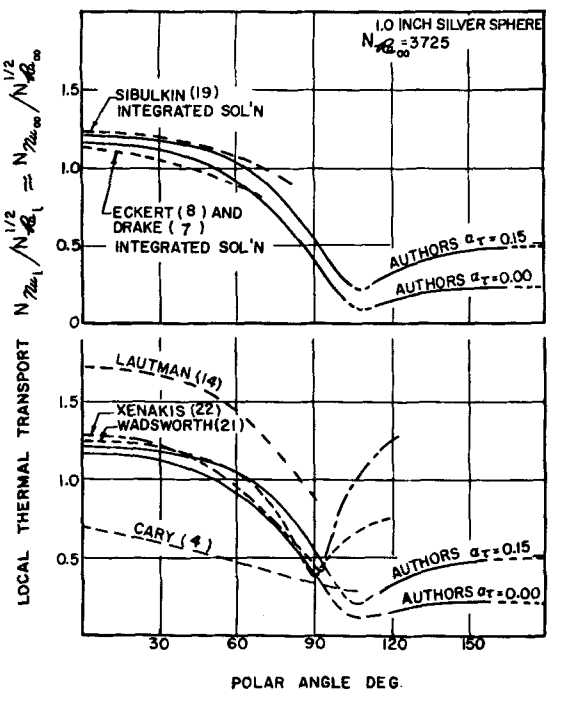

Fig. 7. Comparison of local thermal transfer from several sources.

is with thermal transport alone. The standard error of estimate of the experimental data from the smoothed curves for the 1.0-in. porous sphere was 1.06 and for the 1.0-in. silver sphere was 0.63. In Table 3 smooth values of the macroscopic Nusselt number for conditions at the surface are set forth for even values of Reynolds number. Again it is apparent that the values of Nusselt number for combined thermal and material transport are markedly higher than the values for thermal transport alone.

In Figure 4 the effect of apparent turbulence level upon the relative macroscopic thermal transport from the porous and silver spheres is shown. Within the uncertainty of measurement and at the rates of material transport encountered the effect of turbulence is the same upon the thermal transport to the porous sphere and from the silver sphere.

The distribution of normalized surface temperature, which is described in Equation (8), is available in tabular form for the 1.0-in. porous sphere (*20*). These data have been smoothed with respect to polar angle and conditions of flow. The standard error of estimate of the experimental data from the smoothed values is 0.0071. An example of temperature traverse data for the 1.0-in. silver sphere, presented as a function of horizontal and vertical distance, is also available (*20*), as are values of the normalized wire temperature for the silver sphere (*20*).

Data concerning the relative local transport for a 1.0-in. silver sphere as a function of apparent level of turbulence, Reynolds number, and polar angle is portrayed graphically in Figures 5, 6, and 7, as well as in tabular form (*20*). The actual local transport for the 1.0-in. silver sphere determined from the information presented in Table 3 is presented in Figure 5 as a function of apparent level of turbulence for a Reynolds number of 3,725. The value of the macroscopic Nusselt number for these conditions is also included.

The influence of level of turbulence upon thermal transport at stagnation for the 1.0-in. silver sphere is presented in Figure 6 for three values of Reynolds number. The predicted values for zero level of turbulence which are available from the work of Sibulkin (*18*), Frössling (*9*), and Korobkin (*13*) are included. The agreement of the experimental and theoretical values seems satisfactory. In relation to the experimental values there exists some question concerning the temperature at which the properties of the fluid should be chosen for the calculation of $N_{Nu}/N_{Re}^{1/2}$. However the effect of this choice, within the range of temperatures encountered in these studies, is almost negligible provided all the arbitrary properties of the fluid are taken at one temperature. This may be seen from the equation

$$\frac{N_{Nu}}{N_{Re}^{1/2}} = \left[\frac{\mathrm{d}\, k_i \left(\frac{\partial t}{\partial r}\right)_{r=0}}{k\,(t_i - t_\infty)}\right] \left[\frac{1}{\sqrt{U_\infty\, \mathrm{d}/\nu}}\right] = \left[\frac{k_i \left(\frac{\partial t}{\partial r}\right)_{r=0}}{(t_i - t_\infty)} \sqrt{\frac{\mathrm{d}}{U_\infty}}\right] \left[\frac{\sqrt{\nu}}{k}\right] \quad (10)$$

where the last factor $\sqrt{\nu}/k$ includes the arbitrarily chosen fluid properties. This factor may be shown to be nearly constant for air for a wide range of temperatures. Values which appear in Figure 6 were calculated by means of the molecular properties at the temperature of the interface. The theoretical values (*9, 13, 18*) are based upon constant values of the molecular properties in the boundary flow.

Figure 7 portrays the influence of polar angle upon the local Nusselt number. Again to permit direct comparison with calculated and experimental values obtained by others, both the Nusselt number and Reynolds number are based on the molecular properties at the temperature of the interface. Satisfactory agreement with the calculated values of Sibulkin (*19*), Eckert (*8*), and Drake (*7*) at polar angles below 90 deg. was obtained. The experimental measurements of Xenakis (*22*) and Wadsworth (*21*) also agree well with the current data up to separation, which occurs at a somewhat smaller polar angle than was experienced in this study. The data of Lautman (*14*) and Cary (*4*) are not in satisfactory agreement with the present data or with the measurements of Xenakis (*22*) and Wadsworth (*21*).

The rapid decrease in the Nusselt number with increase in the polar angle continues with the growth of the boundary layer until separation is reached at about 105 deg. In this region where vortices are being shed by the sphere, conditions are far from steady and the uncertainties of meas-

TABLE 3. MACROSCOPIC NUSSELT NUMBER, $N^*_{Nu_i}$

Reynolds number	1.0-in. porous sphere uncorrected*	1.0-in. porous sphere corrected†	1.0-in. silver sphere
	$\alpha_T = 0$		
2,000	31.3	29.0	22.7
3,000	37.9	35.5	27.9
4,000	43.6	41.2	32.2
5,000	48.5	46.1	36.0
6,000	52.8	50.5	39.4
7,000	56.9	54.6	42.7
8,000	60.6	58.5	45.7
	$\alpha_T = 0.05$		
2,000	31.9	29.5	23.1
3,000	38.9	36.4	28.6
4,000	45.0	42.5	33.2
5,000	50.1	47.8	37.3
6,000	54.8	52.5	41.1
7,000	59.2	56.9	44.7
8,000	63.2	61.1	48.1
	$\alpha_T = 0.10$		
2,000	33.0	30.6	23.9
3,000	40.6	38.3	30.1
4,000	47.3	45.3	35.3
5,000	53.3	51.4	40.0
6,000	58.6	56.9	44.3
7,000	63.6	62.1	48.6
8,000	68.2	67.0	52.6
	$\alpha_T = 0.15$		
2,000	36.0	33.2	26.1
3,000	45.9	42.8	33.6
4,000	55.3	52.0	40.4
5,000	64.3	61.1	47.0
6,000	73.1	70.0	53.4
7,000	82.3	79.2	60.0
8,000	91.4	88.8	66.4

* Uncorrected for radiant transport.
† Corrected for radiant transport.

urement are much larger than in the forward hemisphere. This accounts for the dotted portions of the curve in Figure 7. At higher polar angles the boundary flows become more stable and the Nusselt number increases as shown in Figure 7.

It should be recognized that no direct measurements of the scale of the turbulence was made. Undoubtedly changes in the scale of the turbulence will modify the effect of the intensity of the turbulence on the transport phenomena. It was beyond the objectives and scope of the current investigation to undertake a study of the effect of the scale of turbulence on the material and thermal transport from spheres.

ACKNOWLEDGMENT

This experimental work was conducted with the financial support of the Peter E. Fluor Memorial Fellowship, and Emilio Venezian was the recipient of this fellowship. Lorine Faris and Ann Taylor assisted with the calculations and with the preparation of the manuscript, respectively.

NOTATION

A = area, sq.ft.
C_p = isobaric heat capacity, B.t.u./(lb.)(°F.)
$\mathbf{d}$ = diameter of sphere, in. or ft.
d = differential operator
E = electromotive force, v.
$\overset{\circ}{H}$ = enthalpy, B.t.u./lb.
h = heat transfer coefficient, B.t.u./(sec.)(sq.ft.)(°F.)
I = current, amp.
k = thermal conductivity, B.t.u./(sec.)(sq.ft.)(°F./ft.)
L = latent heat of vaporization, B.t.u./lb.
$\overset{\circ}{m}$ = evaporation rate, lb./(sec.)(sq.ft.)
$\overset{\circ}{\mathbf{m}}$ = total material transfer rate from surface, lb./sec.
N_{Nu} = Nusselt number
$\overset{\circ}{Q}$ = local thermal flux from surface, B.t.u./(sec.)(sq.ft.)
$\overset{\circ}{\mathbf{Q}}$ = total thermal transfer rate from surface, B.t.u./sec.
r = radial distance normal to surface of sphere, in. or ft.
N_{Re} = Reynolds number
T = thermodynamic temperature, °R.
t = temperature, °F.
U = gross velocity, ft./sec.
x = distance along supporting tube, in. or ft.

Greek Letters

α_T = apparent longitudinal turbulence level, fraction
β = Stefan-Boltzmann constant, 0.04758×10^{-11}, B.t.u./(sec.)(sq.ft.)(°R.)^4
ϵ = emissivity
θ = time, sec.
ν = kinematic viscosity, sq.ft./sec.
ξ = total energy flux, B.t.u./sec.
$\overline{\mathbf{T}}$ = nondimensional temperature ratio
ψ = polar angle measured from stagnation point, deg.
∂ = partial differential operator

Subscripts

e = electrical energy
eq = equator
g = gas phase
i = solid-gas or gas-liquid interface
k = n-octane
l = liquid phase
o = zero turbulence level
r = radiation
sp = sphere
sr = surroundings
t = supporting tube
w = thermocouple wires
∞ = free stream

Superscript

* = surface average

LITERATURE CITED

1. Bathish, L. N., and B. H. Sage, *A.I.Ch.E. Journal*, **6**, 693 (1960).
2. Brown, R. A. S., Kazuhiko Sato, and B. H. Sage, *Ind. Eng. Chem., Chem. Eng. Data Series*, **3**, 263 (1958).
3. Brown, R. A. S., and B. H. Sage, *J. Chem. Eng. Data*, **6**, 355 (1961).
4. Cary, J. R., *Trans. Am. Soc. Mech. Engrs.*, **75**, 483 (1953).
5. Davis, Leo, *Rept. 3-17*, Jet Propulsion Laboratory, Calif. Inst. Technol, Pasadena, California (1952).
6. ———, *Rept. 3-22*, Jet Propulsion Laboratory, Calif. Inst. Technol, Pasadena, California (1950).
7. Drake, R. M., Jr., *J. Aeronaut. Sci.*, **20**, 309 (1953).
8. Eckert, Ernst, *VDI-Forschungsh.* No. 416, *Beil. Forsch. Gebiete Ingenieurw.*, No. 13B, p. 1 (1942).
9. Frössling, Nils, *Lunds Univ. Arsskr.*, N. F. Avd 2, band 36 (1940); *Natl. Advisory Comm. Aeronaut. Tech. Memo 1432* (1958).
10. Hsu, N. T., H. H. Reamer, and B. H. Sage, Document 4219, Am. Doc. Inst., Washington 25, D. C. (1954).
11. Hsu, N. T., and B. H. Sage, *A.I.Ch.E. Journal*, **3**, 405 (1957).
12. Hsu, N. T., Kazuhiko Sato, and B. H. Sage, *Ind. Eng. Chem.*, **46**, 870 (1954).
13. Korobkin, Irving, *Am. Soc. Mech. Engrs., Paper 54-F-18 Revised*, Am. Soc. Mech. Engrs. Milwaukee Meeting, Milwaukee, Wisconsin (September, 1954).
14. Lautman, L. G., and W. C. Droege, *Rept. No. AIRL A6118*, Air Materiel Command, 50-15-3 (August, 1950).
15. Rossini, F. D., et al., "Selected Values of Physical and Thermodynamic Properties of Hydrocarbons and Related Compounds," Carnegie Press, Pittsburgh, Pennsylvania (1953).
16. Sato, Kazuhiko, and B. H. Sage, *Trans. Am. Soc. Mech. Engrs.*, **80**, 1380 (1958).
17. Short, W. W., R. A. S. Brown, and B. H. Sage, *J. Appl. Mechanics*, **27**, 393 (1960).
18. Sibulkin, Merwin, *J. Aeronaut. Sci.*, **19**, 570 (1952).
19. ———, "Theoretical Solutions for Heat Transfer on a Sphere," reported in reference *13*, unpublished (1952).
20. Venezian, Emilio, Manuel J. Crespo, and B. H. Sage, Document 7159, Am. Doc. Inst., Washington 25, D. C., (1962). $2.50 for photoprints or $1.75 for 35-mm. microfilm.
21. Wadsworth, J., *Report No. MT-39*, National Research Council of Canada, Division of Mechanical Engineering (September 12, 1958).
22. Xenakis, G., A. E. Amerman, and R. W. Michelson, *WADC Tech. Rept. 53-117*, Wright Air Development Center, Dayton, Ohio (April, 1953).

Manuscript received June 6, 1961; revision received November 22, 1961; paper accepted November 22, 1961. Paper presented at A.I.Ch.E. Los Angeles meeting.